Title
MOLECULAR PHOTOEMISSION AT 132.3 eV. THE SECOND-ROW HYDRIDES

Authors
Banna, M.S.
Shirley, D.A.

Publication Date
1975-03-01

Submitted to Journal
of Chemical Physics

LBL-3478
Preprint

MOLECULAR PHOTOEMISSION AT 132.3 eV. THE SECOND-ROW HYDRIDES

M. S. Banna and D. A. Shirley

March 1975

Prepared for the U. S. Energy Research and
Development Administration under Contract W-7405-ENG-48

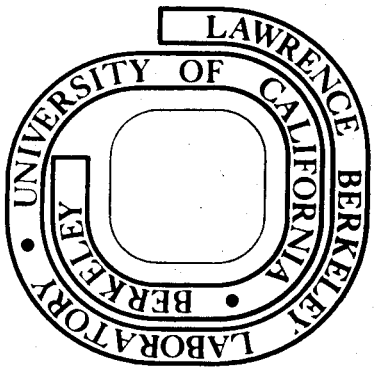

DISCLAIMER

Molecular Photoemission at 132.3 eV. The Second-Row Hydrides*

M. S. Banna† and D. A. Shirley

Department of Chemistry
and Lawrence Berkeley Laboratory
University of California, Berkeley 94720

ABSTRACT

Photoemission spectra of the second-row hydrides CH_4, NH_3, H_2O, and HF, as well as Ne, obtained with ultrasoft (132.3 eV) x-rays from the yttrium Mζ line and with soft x-rays are compared and discussed. The 2s-derived $2a_1$ or 2σ orbitals show large relaxation energies, as do the 2s orbitals in the free atoms. The high binding energies of the $2a_1$ orbitals in CH_4 and NH_3 indicate that much of the bond energy resides in these orbitals. Bond energies estimated from changes in the average valence-electron binding energies from atoms to hydrides show rough agreement with literature values. Relative molecular orbital peak intensities show dramatic changes from 132.3 eV to 1253.6 eV photon energies, with the atomic cross-section ratio 2p/2s near unity at 132.3 eV and near 0.1 at 1253.6 eV. This difference allows peaks to be assigned to molecular orbitals in some cases by visual inspection, on the basis of atomic orbital composition. Comparison with theoretical intensities based on plane-wave or OPW continum final states shows qualitative agreement, proving the diagnostic value of this approach, but quantitative agreement will require more theoretical work. Values of $\sigma(2p)/\sigma(2s)$ for atomic C, N, O, F, and Ne were derived from the spectra at both photon energies.

I. Introduction

The 10-electron second-row hydrides HF, H_2O, NH_3, CH_4 comprise an instructive series for the study of electronic properties in the 1-10 eV energy range. On this scale some subtleties of molecular geometry are blurred over, and these hydrides can be regarded as being derived from atomic neon by moving 1-4 protons from the nucleus to the atomic periphery. The attendant reduction in strength of the central potential is manifest particularly in the variation of orbital binding energies, as well as other properties.

Further removal of the protons would lead to dissociation into neutral atoms[1]. Reversing this path, the hydrides may be regarded as being formed from atoms of the corresponding second-row elements by bringing up hydrogen atoms from infinity. According to this picture vestigal atomic properties should be perceptible in the electronic structures of the hydrides. Of course these properties must be sought on an energy scale of 1-10 eV. Again orbital binding energies provide convenient indicators of the connection between atoms and their hydrides.

This paper deals with the binding energies of the electronic orbitals in Ne, HF, H_2O, NH_3, and CH_4 as determined by x-ray photoemission spectroscopy (XPS) using soft ($\sim 10^3$ eV) and ultra-soft ($\sim 10^2$ eV) x-rays. Relative intensities of the peaks in the XPS spectra are interpreted in terms of the atomic orbital composition of each molecular orbital. The characteristic Mζ x-rays from an yttrium anode were especially useful in this regard, because the 2p/2s photoionization cross section ratio changes dramatically between this photon energy (132.3 eV) and that of the $MgK\alpha_{12}$ transition (1253.6 eV). We have measured the Mζ XPS spectra of CH_4, NH_3, H_2O, HF, and Ne. The Ne spectrum has been reported earlier by Krause[2],

and our CH_4 and HF spectra have been reported previously in a paper on the fluorinated methanes.[3] The H_2O and NH_3 results are new. We also report a ZrMζ (151.4 eV) XPS spectrum for NH_3. The soft-XPS spectra of all five species are used for comparison. Most of these are now available in the literature,[4,5] from which we obtained data for CH_4, HF, and H_2O.[6] We report MgKα spectra for Ne[7] and NH_3.

Experimental procedures are given in Section II. Binding energies are discussed in Section III, with special reference to trends along the series. Similarities to the corresponding atomic binding energies are noted. Finally, Section IV deals with changes in relative orbital cross sections between 132.3 eV and 1253.6 eV.

II. Experimental

The gases were purchased from Matheson Gas Company and studied at 10^{-2} torr pressure in the Berkeley Iron-Free Photoelectron Spectrometer,[8] modified to accommodate an yttrium source. The x-ray tube design is described fully elsewhere.[9] Oxidation of the yttrium surface led to broadening of the photoelectron lines in some cases. However, it was always possible to distinguish the individual levels and to least-squares fit the peaks without constraining the linewidths (such a constraint can alter the area ratios in some cases). Our experimental peaks were found to be well-represented by Lorentzians[10] in all but one case, the MgKα spectrum of ammonia, for which gaussians were used. All area ratios were computed after eliminating the contributions due to satellite x-rays.[2] Our curve-fitting program also applies a point-by-point correction for the change in spectrometer transmission with energy. Counts were obtained at increments of ~0.3 eV with MgKα (MO region) and ~0.2 eV with YMζ.

The spectra of methane and hydrogen fluoride were shown in Reference 7. The MgKα, YMζ, and ZrMζ spectra of ammonia are shown in Fig. 1. In the

YMζ spectrum, a troublesome interfering structure was observed between the two outer orbitals. Water has intense peaks in that region (Figure 2), but it was eliminated by maintaining the sample at dry-ice temperature throughout the experiment. The kinetic energy of the electrons in the interfering band is ~119 eV. When this is added to the nitrogen 1s binding energy of ammonia (405.6 eV)[4] an x-ray energy of ~525 eV is obtained. Thus the most likely interpretation is that the oxide layer on the yttrium surface produces oxygen Kα x-rays which eject N1s electrons with kinetic energy falling in the MO region obtained with YMζ x-rays. Future workers with yttrium and other oxidizable anodes should be aware of this type of interference. Fortunately, in this case the peaks could be distinguished enough to allow reliable deconvolution. This mechanism was confirmed by using 151.4 eV ZrMζ x-rays (Figure 1), which had the effect of shifting the interfering structure to where it sould overlap with the $2a_1$ peak of NH_3.

One other experimental problem arose. The characteristic $K\alpha_{12}$ radiation of magnesium is accompanied by $K\alpha_{34}$ satellites of 10 eV higher energy. This leads to corresponding peaks in the photoemission spectrum. When the satellites from a strong line coincide in energy with a weak line, the accuracy with which the position and intensity of the latter can be determined is decreased. In this work the $1t_2$ peak in the methane spectrum and the 1e peak in the ammonia spectrum were thus affected.

The MgKα and YMζ of water are shown in Figure 2. The former was reproduced from the work of Siegbahn *et al.*[4,6] Neon spectra are shown in Figure 3.

III. Binding Energies

The MgKα spectra were experimentally referenced to the neon 2s line (48.42 eV)[4]. The YMζ spectra were not referenced to a rare-gas standard; instead, one of the ionization potentials measured with MgKα was used to obtain absolute binding energies in each case.

In Table I we compare the XPS binding-energy results with a selection of literature values obtained from ultraviolet photoemission spectroscopy (UPS). The agreement is good in most cases. The largest difference is in the binding energy of the $1e$ level of ammonia. This may be due to the uncertainty introduced by the interfering x-rays discussed above. However, the ZrMζ spectrum (Figure 1) which is free of interference in the outer MO region, also yields a value that is too high (16.54(4)eV). From the UPS measurement,[11] a Jahn-Teller splitting of ~0.5 eV was estimated for the $1e$ peak. We have therefore used two peaks with a fixed separation of 0.5 eV and equal areas to reproduce the $1e$ band. A good fit could also be obtained with one peak. Both types of fit yielded the same binding energy. The most likely explanation for the discrepancy between the XPS and UPS measurements is the uncertainty of locating the mean of a peak with such a flattened summit. Another intriguing possibility is that the intensity ordering of the two Jahn-Teller states may have changed in going from uv to x-ray exciting photons. This would explain the higher XPS binding energy value since the vertical I.P. obtained by UPS corresponds to the outer, more intense state.

The binding-energy systematics yield information about bonding, as well as about relaxation during the photoemission process. To separate these effects we have included in column 6 of Table I a complete set of orbital energies ϵ from the calculation of Snyder and Basch.[12] Column 7 lists "relaxation energies", E_R, obtained by the relation

$$E_B = -\epsilon - E_R \quad . \tag{1}$$

The relaxation energy so defined absorbs correlation and relativistic contributions as well as relaxation effects <u>per se</u>. Column 9 lists atomic binding energies, averaged over multiplets,[13] taken from calculations by Wilson.[14] Column 10 gives values of relaxation energies for the atomic

orbitals, as given by Gelius[15]. We shall use these highly-reliable calculated results for free atoms in making comparisons as if they were experimental quantities.

The 1s binding energies in atoms and hydrides are very similar, with the hydride values being lower by 0.3% in HF vs. F, 1.0% in H_2O vs. O, 1.2% in NH_3 vs. N, and 1.9% in CH_4 vs. C. Because the total relaxation energy accompanying 1s photoemission is identical to within less than 1eV for each element in the atom and as a hydride, the lower 1s binding energies in the hydrides must be attributed to additional repulsion at the 1s orbitals in the initial states. The 1s orbitals are slightly "reduced" by addition of valence electrons to fill the n = 2 octet.

Turning to the valence shell, it is convenient to divide the peaks into two groups. The most tightly-bound orbital in each molecule has $2a_1$ or 2σ symmetry. It is derived mostly from the 2s shell in a bonding combination. Again E_R is similar for each element in the hydride and free atom. A similar observation was made earlier for the F(2s)-derived orbitals in fluorinated methanes.[5] A striking feature of the present data is the <u>increase</u> in binding energy of this orbital in the hydrides over the 2s orbitals in the free atoms. Such an increase signals stabilization by bond formation. Furthermore, E_B(hydride)-E_B(atom) varies in the order $CH_4 > NH_3 > H_2O > HF$, with the HF value being slightly negative. These two observations can be related to the chemist's simple picture of bond energy residing partly in overlap of the s orbitals with ligand functions. In Figure 4 we have plotted for these hydrides the total bond energy and twice the excess binding energy of the 2σ or $2a_1$ orbital, to see whether an appreciable fraction of the total bond energy might be attributed in this simple picture to this orbital. The data suggest that the bond energy arises largely from $2a_1$ orbitals in

CH_4 and NH_3. The situation for H_2O and HF is less clear. In O and F the 2s orbitals are more tightly bound: admixture of H orbitals may not give a net increase in binding energy. This must not be interpreted entirely in terms of 2s vs. 2p bond character, because except in CH_4 the comparable orbitals can contain small admixtures of p orbitals. There is a trend toward higher <u>total</u> overlap of 2s orbitals with hydrogen from HF to CH_4, brought about partly because the number of hydrogens increases and partly by the trend for the 2s and 2p orbitals to be more nearly degenerate in the lighter elements.

A more conventional molecular orbital diagram for methane is shown in Figure 5. Here we have plotted orbital binding energies for C, H, and CH_4. This type of plot is completely empirical: it employs data from Table I and the H(1s) ionization potential of 13.6 eV. It would be impossible from these data alone to calculate a C-H bond energy. If we just empirically add up all the orbital bonding energies times the orbital populations, however, and assign the difference in average bonding energy of all eight valence electrons to the four C-H bonds in CH_4, this gives a bond-energy estimate of

$$1/4\ [2E(a_1) + 6E(t_2) - 4E(H1s) - 2E(C2s) - 2E(C2p)] = 4.97\ \text{eV}, \qquad (2)$$

in fair agreement with the experimental value of 4.29 eV.[16] The corresponding values for the other hydrides are: NH_3, 3.88 eV vs. 4.05 eV;[16] H_2O, 2.24 eV vs. 4.80 eV;[16] HF, 4.32 eV vs. 5.84 eV.[16] Thus the photoemission spectrum can in most of these cases give a rough idea of bond strength.

In the less tightly-bound molecular orbitals the relaxation energies E_R are usually small, in agreement with the observation that orbital energies usually give the correct ordering of ionization energies. It is interesting that larger values of E_R are observed for the lone "pair" orbitals, $1b_2$ in H_2O and 1π in HF. This would be consistent with a large amount of electron polarization to screen a localized hole.[17] However,

the uncertainty about the value of $E_R(2p)$ in atoms (see Table I) precludes a definitive conclusion.

IV. Intensity Ratios

The differential cross section for producing photoelectrons in the solid angle $d\Omega$ by photons of energy $\hbar w$ is given by[18]

$$\frac{d\sigma}{d\Omega} = \frac{\pi e^2}{m^2 c\omega} \left| \underset{\sim}{u} \cdot \langle \Psi_o | \sum_n \underset{\sim}{p}_n | \Psi_j \rangle \right|^2 \rho \qquad (3)$$

Here Ψ_o is the initial state, Ψ_j the final state upon ionization; $\underset{\sim}{u}$ is a unit vector in the photon polarization direction; $\underset{\sim}{p}$ is the linear momentum operator for the n^{th} electron; and $\rho(E)$ is the density of final states with energy near E. For randomly oriented molecules, the expression must be averaged over all directions. An average must also be taken over all orientations of $\underset{\sim}{u}$ if the radiation employed is not polarized. The final expression has the general form[19]

$$\left\langle \frac{d\sigma}{d\Omega} \right\rangle_{Av} = (\sigma/4\pi)[1 - 1/4\beta(3\cos^2\theta - 1)] \qquad (4)$$

where σ is the total cross section (cross section for electron emission in all directions), β is the asymmetry parameter and θ is the angle between the direction of the exciting radiation and the direction of photoelectrons in the solid angle $d\Omega$. In the present work, only photoelectrons emitted perpendicular to the direction of the unpolarized photon beam were monitored ($\theta = 90^\circ$). Thus the reported cross-sections are related to $\sigma_\perp$, which is given by

$$\sigma_\perp = (\sigma/4\pi)\ (1 + 1/4\ \beta),\ \theta = \pi/2. \qquad (5)$$

σ_l's of the MO's of a certain system were measured relative to one another, both at the YMζ and MgKα_{12} energies.

Ellison[19] derived expressions for $\langle \frac{d\sigma}{d\Omega} \rangle_{Av}$ assuming a plane wave (PW), or a plane wave orthogonalized to all the filled bound orbitals (OPW), for the continuum final state. He also assumed that the bound orbitals did not change upon ionization (frozen-orbital approximation). The expressions thus derived were employed by Debies and Rabalais[20] to compute cross sections and angular distributions for neon and the second-row hydrides at various photon energies. Debies and Rabalais used ab initio molecular wavefunctions with minimal bases of non-orthogonal real Slater-type orbitals for the bound states. Orbital exponents were determined following Slater's rules.

The simplifying assumptions of a plane wave continuum state and frozen passive orbitals were used by Gelius[21] to derive an approximate expression for the molecular orbital cross section:

$$\sigma_i \text{ (MO)} \cong \sum_j P_{ij} \sigma_j \text{ (AO)}. \qquad (6)$$

Here P_{ij} is the electron population of AO ϕ_j in molecular orbital i. Equation (4) was derived for cross sections at x-ray energies above ~ 1000 eV. The same expression was used by Banna and Shirley[3] to analyze the fluoromethane spectra obtained with YMζ radiation (132.3 eV). Encouraged by the good agreement obtained there and elsewhere[5], we shall use the Gelius model to analyze the relative peak intensities in the hydrides.

The qualitative change in relative cross sections when the exciting source is changed from MgKα to YMζ is best illustrated by referring to the neon spectrum (Figure 3). A dramatic increase in the 2p/2s intensity ratio occurs at low photon energy. This behavior can be explained qualitatively by considering the one-electron momentum matrix element,

$$\langle \chi_f(j) \mid \underset{\sim}{p}_j \mid \phi_i(j) \rangle, \qquad (7)$$

where $\phi_i(j)$ and $\chi_f(j)$ denote, respectively, the initial bound state and final continuum state for electron j. Under the assumption that the final state is formed upon ionization by promoting electron j from a bound to a continuum orbital orthogonal to the occupied MO's, while leaving the remaining electrons unchanged, equation (3) reduces to a quantity proportional to the square of the matrix element (7). When the deBroglie wavelength of the outgoing electron is such as to 'match' the curvature of the orbital $\phi_i(j)$, the cross section would be expected to be large. In terms of this overlap picture, discussed by Price et al.[22], it becomes clear why high-energy (~ 1000 eV) radiation yields a high intensity for 2s orbitals relative to 2p orbitals, while the reverse is true with ~100 eV radiation. We have noted previously[3] that this trend is observed in the fluorinated methanes as well as methane and hydrogen fluoride. The spectra of water and ammonia provide further support for the overlap argument (Figures 1 and 2). The $1b_2$ orbital of water, which is purely 2p in character, gains substantially in intensity relative to the 2s-like $2a_1$ orbital at the YMζ energy of 132.3 eV. The 2p contributions to $3a_1$ and $1b_1$ also result in an intensity increase, but the presence of some s character in $3a_1$ makes this increase less dramatic than for $1b_2$. Interestingly, $1b_1$ retains roughly the same intensity relative to $1b_2$ in going from MgKα to YMζ. This behavior would not be expected on the basis of 2p populations alone, since $1b_2$ is totally 2p in character while $1b_1$ is only 60% 2p and 40% hydrogen 1s. One possible explanation is that the hydrogen 1s cross section increases faster than the oxygen 2p cross section when the photon energy is changed from 1254 eV to 132 eV. Another more likely explanation is that, since $1b_1$ is strongly O-H bonding[12], its diffuse electronic

population overlaps with the outgoing electron better at 132 eV, thus resulting in a cross section that is higher than would be expected on the basis of the 2p population alone. Similarly in ammonia, one of the 1e orbitals is strongly N-H bounding.[12] From Figure 1 it can be seen that 1e becomes more intense than $3a_1$ at YMζ (or ZrMζ) energy even though $3a_1$ is 90% 2p while 1e is only 60% 2p.[12] Both 1e and $3a_1$ gain with respect to $2a_1$ at low photon energy, as expected.

In columns 4,6,8, and 9 of Table II we compare respectively the relative peak intensities at 21 eV(HeI), 41 eV(HeII), 132 eV(YMζ), and 1254 eV ($MgK\alpha_{1,2}$) exciting photon energies. The values for YMζ and MgKα are also plotted in Figure 6. From Table II, it is seen that the relative intensities obtained with the helium resonance lines are generally quite similar to the values obtained with YMζ. This observation is in line with the overlap picture discussed above, since, as with YMζ, the wave lengths of electrons ejected with the helium lines match 2p orbitals better than 2s.

The theoretical photoionization cross sections of Debies and Rabalais[20] at 132 eV and 1254 eV are shown in columns 5 and 7, respectively. The computations correctly predict that the intensity ordering of the $2a_1$ and $1t_2$ levels of methane is reversed in going from the MgKα to the YMζ excitation energy (Figure 6). The correct intensity ordering at 1254 eV is also predicted for ammonia. However, at the YMζ energy, $3a_1$ is calculated to have a slightly higher intensity than 1e, contrary to the experimental result. Similarly, the calculation reverses the intensity order of the other two MO's of water at 132 eV. It is interesting to note that if peak <u>heights</u> were compared instead of peak areas, the calculations would yield the correct intensity ordering, both in water and

in ammonia. In HF, however, the wrong order is predicted for the outer two MO's at the MgKα energy. The theoretical fluorine 1s intensity also compares poorly with the experimental value. Finally, the neon 2p/2s relative intensity agrees very well with experiment, both at 132 eV and 1254 eV excitation energies.

Fadley[23] has shown that the assumption that the orbitals of the ion remain frozen during ionization, used in these present calculations, leads to cross sections which include the probability for multiple-as well as single-electron excitations. In the case of the hydrides, one observes no intense satellite peaks in the MO region. Core ionization, however, is often accompanied by multiple-electron transitions. In hydrogen fluoride, for example, the probability for multiple-electron transitions is ~ 20% of the probability for single-electron ionization.[24] The core spectrum of neon is known to contain discrete satellites totalling ~ 12% of the main line.[25] Addition of multiple-electron intensities to the core intensities of these two systems widens the gap between the experimental and theoretical ratios. Absolute experimental subshell cross-sections are available for neon.[26] (See Table III). The calculations of Debies and Rabalais underestimate the neon 1s cross section without adding the shake-up contributions. The 2p and 2s cross-sections are overestimated, which means that including the multiple-electron transitions should improve the agreement. From the work of Wuilleummier and Krause,[27] it is known that shake-up probabilities amount to ~ 5% the intensity of each of 2p and 2s at the YMζ energy, ~ 11% and ~ 6% of 2p and 2s, respectively, at the MgKα energy.

In general, the theoretical results are in better agreement with

experiment at 1254 eV than at 132 eV. This is not surprising, because the plane-wave approximation becomes better at higher electron energy. For all the hydrides as well as neon, the intensity ratio of the 2p-like to the 2s-like orbitals seems to be overestimated at the YMζ energy and underestimated at the MgKα energy.

With the Gelius model (eq. 6) it is possible to obtain semiempirical $\sigma_1(2p)/\sigma_1(2s)$ ratios for the central atoms of the hydride series. Using gross populations calculated from the wavefunctions of Snyder and Basch[12] and the experimental area ratios listed in Table II, we have estimated relative intensities $\sigma_1(2p)/\sigma_1(2s)$ at both YMζ and MgKα energies. The hydrogen 1s cross section was taken to be zero. For each hydride one area ratio of two MO's is needed to obtain σ_{2p}/σ_{2s}. The values listed in Table IV represent the average of the atomic cross-section ratios calculated using the area of $2a_1$ relative to each of the remaining MO's. (Only one value is possible for methane since it has only two MO's).

The ratios at the MgKα energy indicate that σ_{2p}/σ_{2s} increases in going across the periodic table from carbon to neon. This is supported by the calculations of Huang and Ellison[28,29] and of Nefedov et al.[29] listed in Table IV. The former assume a plane wave for the final continuum state. They employ either Slater-type orbitals orthogonalized to the 1s core,[28] or SCF Clementi atomic orbitals.[29] The latter are in excellent agreement with our semiempirical results. Slater-type orbitals yield ratios that are somewhat smaller than ours, but the agreement is still good. The SCF relativistic Hartree-Fock-Slater calculations of Nefedov et al.[30] (Table IV) represent ratios of total (as opposed to differential) 2p to 2s cross sections. However, as the authors point out,

the correction in this case is small (a factor of 1.00 to 1.08). It must also be noted the oxygen and fluorine ratios of Nefedov et al. were computed for O^- and F^-, respectively, instead of the neutral species. The values listed in Table IV are in good agreement with ours.

At the YMζ photon energy of 132.3 eV. the ratios do not appear to change monotonically with atomic number, but the general trend seems to be the same as that at the MgKα photon energy of 1253.6 eV; i.e., $\sigma_l(2p)/\sigma_l(2s)$ increases with Z. The YMζ values are generally closer to unity than the MgKα values. Thus the YMζ energy seems to fall in a region where the 2p and 2s intensities are about equal.

In conclusion, the relative intensities of the hydride molecular orbital photopeaks at YMζ photon energies, are significantly different than at high photon energies, in ways that can be simply related to atomic orbital composition of the molecular orbitals. The relative intensities are predictable semi-quantitatively using theories based on plane-wave final states, but quantitative agreement will require more theoretical work. Finally, atomic 2p/2s cross-section ratios derived from the hydride photoemission data using certain approximations show an upward trend with atomic number from C to Ne for 1254 eV photons but a minimum at N for 132 eV photons. The former trend agrees well with theoretical predictions.

FOOTNOTES AND REFERENCES

*Work performed under the auspices of the U.S. Energy Research and Development Administration.

+Present address: The University of British Columbia, Department of Chemistry, Vancouver, B.C., Canada.

1. Thus each hydride corresponds to a local minimum in energy on a path in which hydrogen atoms are brought to a second-row atom from infinity, with the proton coalescing into the central nucleus to form neon.

2. M. O. Krause, Chem. Phys. Letters 10, 65 (1971); see also M. O. Krause and F. Wuilleumier, Phys. Letters 35A, 341 (1971).

3. M. S. Banna and D. A. Shirley, Chem. Phys. Letters, to be published.

4. K. Siegbahn, C. Nordling, G. Johansson, J. Hedman, P. F. Hedén, K. Hamrin, U. Gelius, T. Bergmark, L. O. Werme, R. Manne, and Y. Baer, ESCA Applied to Free Molecules, (North-Holland Publishing Co., Amsterdam 1969).

5. M. S. Banna, B. E. Mills, D. W. Davis, and D. A. Shirley, J. Chem. Phys. 61, 4780 (1974).

6. We thank Professor Carl Nordling for permission to reproduce the H_2O spectrum from Figure 5.3.1 of Reference 4. The CH_4 and HF orbital intensities were obtained from Reference 5.

7. Siegbahn, et al., reported Ne spectra. See Ref. 4.

8. C. S. Fadley, S. B. M. Hagstrom, M. P. Klein, and D. A. Shirley, J. Chem. Phys. 48, 3779 (1968).

9. M. S. Banna, Ph.D. Thesis, University of California, Lawrence Berkeley Laboratory, Report No. LBL-3473.

10. This does not imply lifetime broadening: the peak shape arises from several contributions folded together. Other forms of some of these contributions are not known in detail.

11. D. W. Turner, C. Baker, A. D. Baker, and C. R. Brundle, Molecular Photoelectron Spectroscopy, (Wiley-Interscience, London 1970).

12. L. C. Snyder and H. Basch, Molecular Wave Functions and Properties (Wiley, New York, 1972).

13. We thank R. L. Martin, who worked out these average values.

14. R. M. Wilson, J. Chem. Phys. 60, 1692 (1974).

15. U. Gelius, Physica Scripta 9, 133 (1974).

16. L. Pauling, "The Nature of the Chemical Bond", Third Ed. (Cornell University Press, 1960), p. 85.

17. R. L. Martin and D. A. Shirley, J. Amer. Chem. Soc. 96, 5299 (1974).

18. L. L. Lohr, Jr., in Electron Spectroscopy, edited by D. A. Shirley (North-Holland Publishing Co., Amsterdam, 1972) p. 245.

19. F. O. Ellison, J. Chem. Phys. 61, 507 (1974).

20. T. P. Debies and J. W. Rabalais, J. Amer. Chem. Soc. 97, 487 (1975). J. W. Rabalais, T. P. Debies, J. L. Berkosky, J-T. Huang and F. O. Ellison, J. Chem. Phys. 61, 516 (1974).

21. U. Gelius, Ref. 18, p. 311.

22. W. C. Price, A. W. Potts, and D. G. Streets, Reference 18, p. 187.

23. C. S. Fadley, Chem. Phys. Letters 25, 225 (1974).

24. B. E. Mills, private communication.

25. U. Gelius, J. Electron Spectrosc. 5, 985 (1974).

26. F. Wuilleumier, in Advances in X-Ray Analysis 16, edited by B. L. Henke, (Plenum Press, New York 1973) p. 63.

27. F. Wuilleumier and M. O. Krause, Phys. Rev. A10, 242 (1974).

28. J-T. J. Huang and F. O. Ellison, Chem. Phys. Letters 25, 43 (1974).

29. J-T. J. Huang and F. O. Ellison, J. Electron Spectrosc. 4, 233 (1974).

30. V. I. Nefedov, N. P. Sergushin, I. M. Band, and M. B. Trzhaskovskaya, J. Electron Spectrosc. 2, 383 (1973).

TABLE I. Orbital Binding Energies in Four Second-Row Hydrides, and Related Quantities (eV).

Species	Orbital	E_B MgKα	E_B YMζ	E_B HeI,II[a]	$-\varepsilon$[h]	E_R	nl	E_B^A[i]	E_R^A
CH_4[b]	$1t_2$	14.2(2)	14.5(1)	14.0	14.74	0.24	2p	10.79	0.3, 1.6
	$2a_1$	23.05(2)	23.05(3)[g]	23.0	25.68	2.63	2s	17.81	2.4
	$1a_1$	290.8			305.0	14.2	1s	296.5	13.7
NH_3[c]	$3a_1$	11.04(2)	11.04(2)[g]	10.85	11.22	0.18	2p	15.05	
	1e	16.74(6)	16.49(4)	15.8	16.97	0.48			
	$2a_1$	27.74(2)	27.76(5)		31.16	3.40	2s	23.86	3.0
	$1a_1$	405.6[f]			422.3	16.7	1s	410.7	16.6
H_2O[d]	$1b_2$	12.6	12.60(2)[g]	12.61(6)	13.78	1.18	2p	15.66	
	$3a_1$	14.7	14.75(3)	14.73(6)	15.42	0.67			
	$1b_1$	18.4	18.74(4)	18.55	19.52	0.78			
	$2a_1$	32.2	32.61(5)		37.07	4.46	2s	31.54	3.6
	$1a_1$	539.7			559.3	19.6	1s	545.0	19.3
HF[e]	1π	16.12(4)	16.12(4)[g]	16.04	17.50	1.38	2p	17.12	
	3σ	19.89(7)	19.79(5)	19.90	20.50	0.71			
	2σ	39.65(2)	39.30(4)		43.61	4.31	2s	40.02	4.1
	1σ	694.0			715.1	21.1	1s	696.2	22.0
Ne[f]	2p	21.59[k]	21.59[g,k]	21.59[k]	23.14	1.55			
	2s	48.42(5)	48.49(1)		52.52	4.03			
	1s	870.2(1)			891.7	21.5			

a. Vertical ionization potentials.
b. In CH_4, $AlK\alpha_{12}$ (1486.6 eV) rather than $MgK\alpha_{12}$ radiation was used because of interfering satellites. $AlK\alpha_{12}$ energies from Ref. 5; He energies from Ref. 20.
c. HeI energies from Ref. 11.
d. MgKα energies from Ref. 4; He energies from C. R. Brundle and D. W. Turner, Proc. Roy. Soc. A307, 27 (1968).
e. MgKα values from Ref. 5; He values from C. R. Brundle, Chem. Phys. Letters 7, 317 (1970).
f. MgKα energies from Ref. 4.
g. Reference peak.
h. From Ref. n, except neon, from P. S. Bagus, Phys. Rev. 139, A619 (1965).
i. References 13, 14.
j. The 1s and 2s values were given by U. Gelius, Physica Scripta 9, 133 (1974). The 2p values given there do not agree with those calculated by us using the hole-state results from Ref. 14. Both values are given for carbon: the rest are omitted.
k. Weighted mean of $2p_{1/2}$ and $2p_{3/2}$ optical ionization energies. See Appendix D of Ref. 4.

TABLE II. Differential Photoionization Cross Section Ratios at 21.21 eV, 40.8 eV, 132.3 eV, and 1253.6 eV Excitation Energy ($\theta = 90°$).

Molecule	MO	E_B (eV)[a]	I(MgKα) exp	I(MgKα)[b] theo	I(YMζ) exp	I(YMζ)[b] theo	I(HeII)[b] exp	I(HeI)[b] exp
CH_4[c]	$1t_2$	14.2(2)	0.12(2)	0.052	2.69(8)	7.54	7.14	
	$2a_1$[h]	23.05(2)	1.00	1.00	1.00	1.00	1.00	
	$1a_1$	290.8[d]	30(1)	26.41	---	---	---	
NH_3[m]	$3a_1$	11.04(2)	0.20(3)	0.020	0.81(5)	22.27	0.81	0.81
	1e	16.74(6)	0.13(4)	0.038	1.04(4)	18.71	1.54	1.78
	$2a_1$[i]	27.74(2)	1.00	1.00	1.00	1.00	---	---
	$1a_1$	405.6[d]	33(1)	24.11	---	---	---	---
H_2O	$1b_2$	12.6[d]	0.095[f]	0.040	0.92(5)	32.38	0.92	0.92
	$3a_1$	14.7[d]	0.26[f]	0.22	1.04(6)	20.56	0.96	1.08
	$1b_1$	18.4[d]	0.081[f]	0.020	0.70(5)	12.56	0.77	0.92
	$2a_1$[j]	32.2[d]	1.00	1.00	1.00	1.00	---	---
	$1a_1$	539.7[d]	19	19.28	---	---	---	---
HF	1π	16.12(4)	0.24(2)	0.12	2.93(2)	23.30	2.93	
	3σ	19.89(7)	0.19(3)	0.17	1.18(4)	6.33	1.20	
	2σ[k]	39.65(2)	1.00	1.00	1.00	1.00		
	1σ	694.0[e]	34(1)	12.70	---	---		
Ne	2p	21.59[d]	0.42	0.26	7.11(2)	8.20		
	2s[l]	48.42(5)[d]	1.00	1.00	1.00	1.00		
	1s	870.2(1)	28(1)[g]	10.54	---	---		

a. MgKα values for all except $1t_2$ and $2a_1$ of CH_4, which were measured using AlKα.
b. Reference 20. Theoretical results were kindly communicated to us by J. W. Rabalais.
c. AlKα used instead of MgKα. The theoretical ratios are also for 1487 eV photons.
d. Reference 4.
e. B. E. Mills, private communication.
f. Calculated by the authors of Ref. 20 from the spectrum in Ref. 4.
g. Reference 26.
h. The theoretical differential cross section is 1.67×10^2 barns at 1254 eV and 4.68×10^3 barns at 132 eV.
i. The theoretical cross section is 2.92×10^2 barns at 1254 eV and 2.25×10^3 barns at 132 eV.
j. The theoretical cross section is 4.72×10^2 barns at 1254 eV and 2.69×10^3 barns at 132 eV.
k. The theoretical cross section is 7.37×10^2 barns at 1254 eV and 9.70×10^3 barns at 132 eV.
l. The theoretical cross section is 9.13×10^2 barns at 1254 eV and 4.66×10^4 barns at 132 eV. Experimental cross section is 4.74×10^2 barns at 1254 eV and 3.20×10^4 barns at 132 eV. (From Ref. 26). Also see Table III.
m. With ZrMζ, $2a_1$: $1e:3a_1$ ratios of 1.00:1.26(3):0.73(2) were obtained.

TABLE III. Comparison of Experimental and Theoretical Differential Photoionization Cross-Sections of Neon (in barns).

	YMζ(132.3 eV)		MgKα(1253.6 eV)	
Level	$\sigma_\perp$ (exp)[a]	$\sigma_\perp$ (theo)[b]	$\sigma_\perp$ (exp)[a]	$\sigma_\perp$ (theo)[b]
2p	2.01×10^5	3.82×10^5	1.86×10^2	2.41×10^2
2s	3.20×10^4	4.66×10^4	4.74×10^2	9.13×10^2
1s	---	---	1.35×10^4	9.62×10^3

a. From Ref. 23.

b. The results of the calculations of Ref. 20 were communicated to us by J. W. Rabalais.

TABLE IV. Relative Photoelectric Cross Sections $\sigma_{\perp}(2p)/\sigma_{\perp}(2s)$ for Second Row Atoms.[a]

Atom	R^{b} (132.3 eV)	R^{b} (1253.6 eV)	R(STO)[c] (1254 eV)	R(CAO)[d] (1254 eV)	R^{e} (1254 eV)
C	1.16	0.052[f]	0.012	0.048	0.032[f]
N	0.66	0.083	0.023	0.077	0.058
O	0.95	0.11	0.042	0.11	0.070
F	1.39	0.13	0.077	0.17	0.098
Ne	2.37	0.14[g]	0.12	0.25	0.14

a. To take the 2p degeneracy into account, all ratios in this table must be multiplied by 3.
b. Semiempirical ratios calculated using eq.(6). Gross populations were obtained from Ref. 12 and area ratios from Table II.
c. From Ref. 28. Slater-type orbitals were used to represent the occupied orbitals, with 2s orthogonalized to the 1s AO. The continuum state was represented by a plane wave.
d. From Ref. 29. SCF Clementi atomic orbitals used instead of STO's.
e. Theoretical total cross-section ratios using a Hartree-Fock Slater potential (Ref.30). Oxygen and fluorine cross-sections were computed for O^{-} and F^{-} respectively, the rest for the neutral species.
f. Cross section ratio at 1487 eV photon energy.
g. Experimental value.

FIGURE CAPTIONS

Fig. 1. Valence photoelectron spectrum of ammonia with MgKα (top), YMζ (middle) and ZrMζ (bottom) x-rays. The peak to the left of 1e (MgKα spectrum) is a satellite of 2a resulting from $MgK\alpha_{3,4}$ x-rays. The structure between 1e and 3a (YMζ spectrum) and to the left of 2a (ZrMζ spectrum) is due to N1s electrons photoejected by OKα x-rays. Oxygen is a contaminant on the anode surface.

Fig. 2. Valence photoelectron spectrum of water with MgKα (top) and YMζ (bottom) x-rays. The MgKα spectrum is reproduced from Ref. 4.

Fig. 3. Photoelectron spectrum of neon with MgKα (top) and YMζ (bottom) x-rays.

Fig. 4. Total bond energies (filled circles) and 2 $E(2a_1)$ - E(2s), for second-row hydrides.

Fig. 5. An orbital correlation diagram for CH_4, using binding energies in C, H, and CH_4. Note lowering in energy of $2a_1$ orbital.

Fig. 6. Schematic of relative photoelectron peak areas and binding energies obtained from the experimental spectra of the second-row hydrides and neon with MgKα and YMζ x-rays. To facilitate comparison, the innermost MO intensities are shown equal for the entire series at each of the two exciting photon energies.

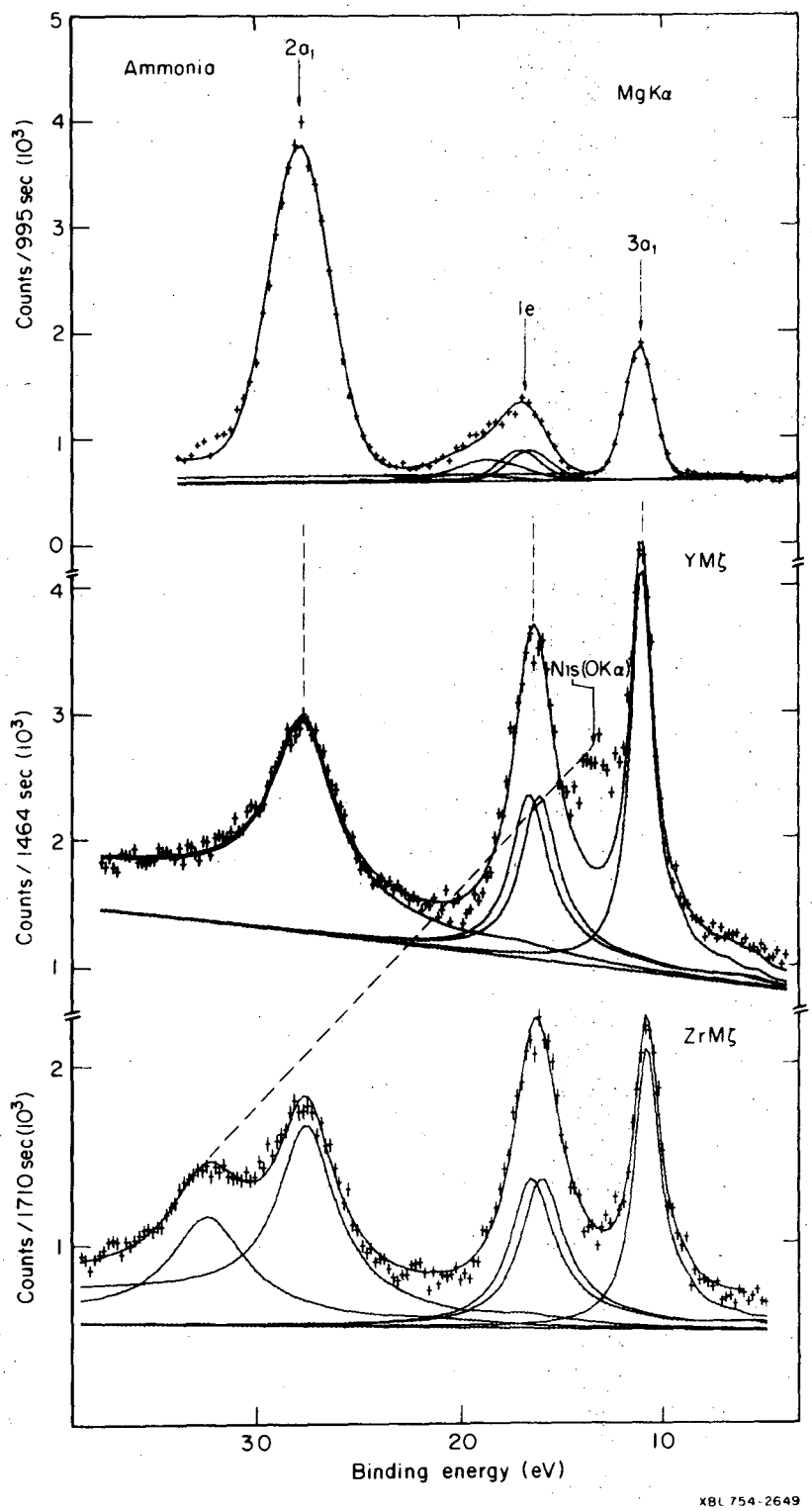
Ammonia
2a1
MgKα
3a1
1e
YMζ
NIs(OKα)
ZrMζ
Counts / 995 sec (10³)
Counts / 1464 sec (10³)
Counts / 1710 sec (10³)
Binding energy (eV)
XBL 754-2649

Fig. 1

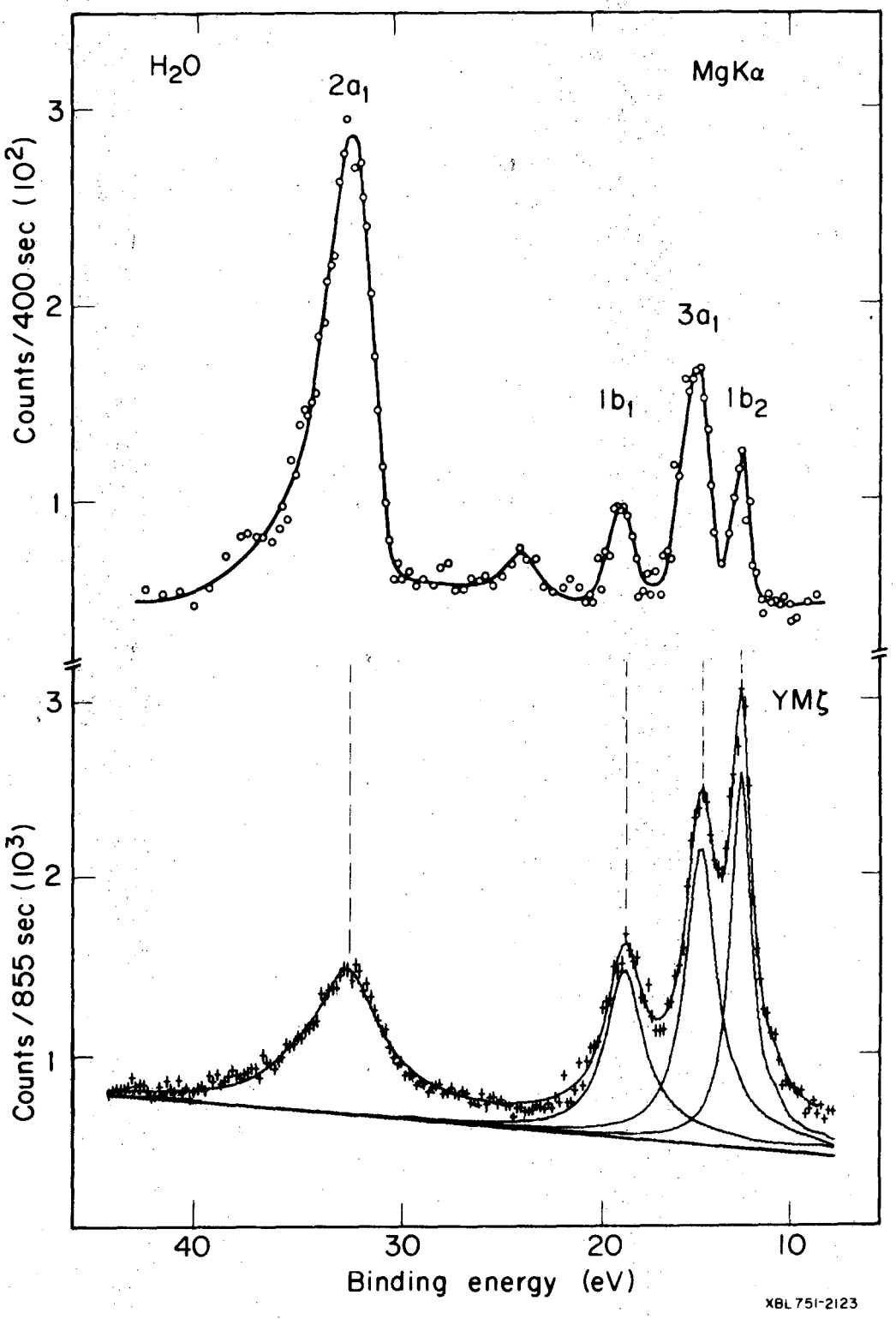

Fig. 2

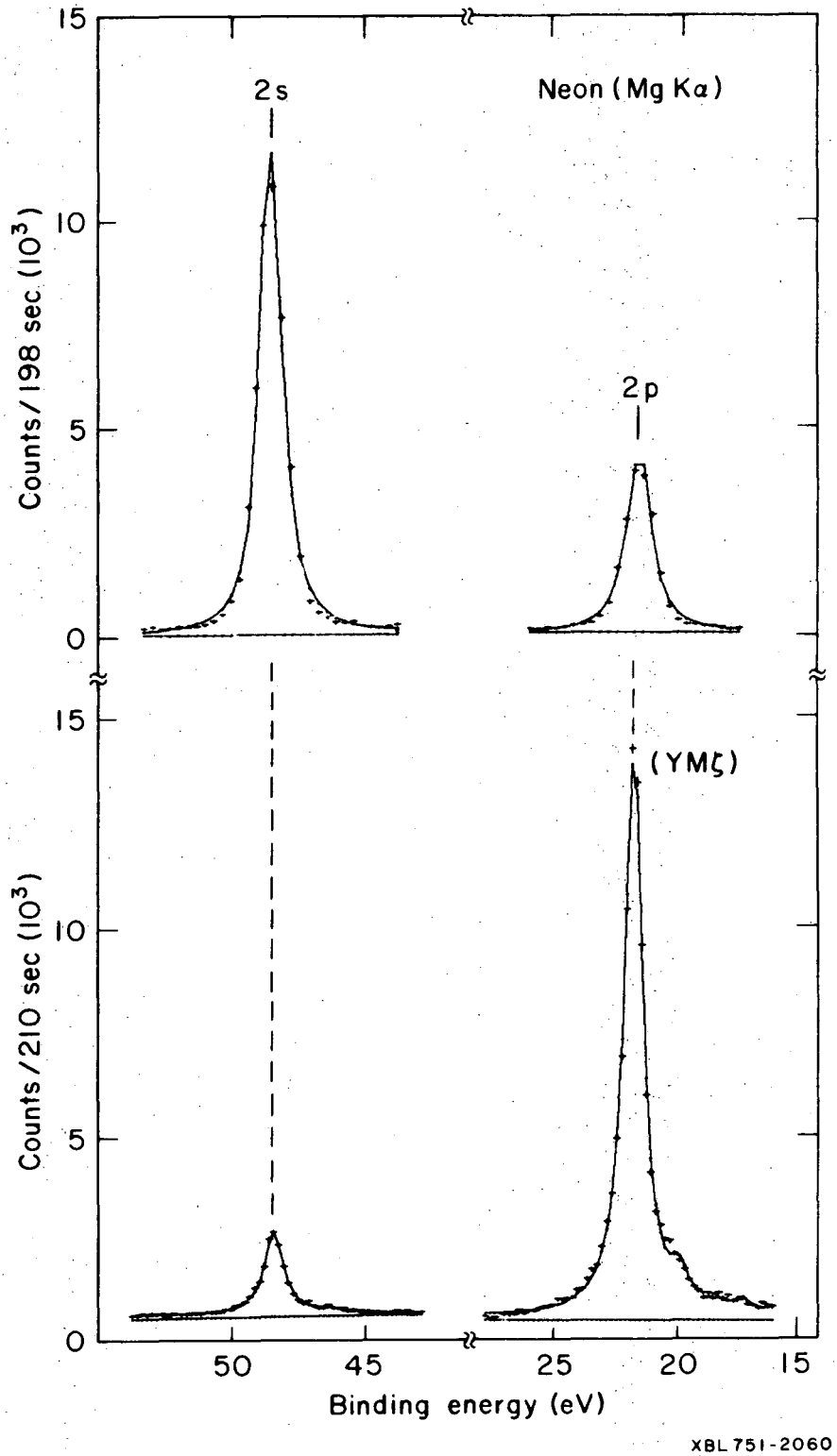
15
10
5
0
2s
Neon (Mg Kα)
2p
Counts / 198 sec (10³)
15
10
5
0
(YMζ)
Counts / 210 sec (10³)
50
45
25
20
15
Binding energy (eV)
XBL 751-2060

Fig. 3

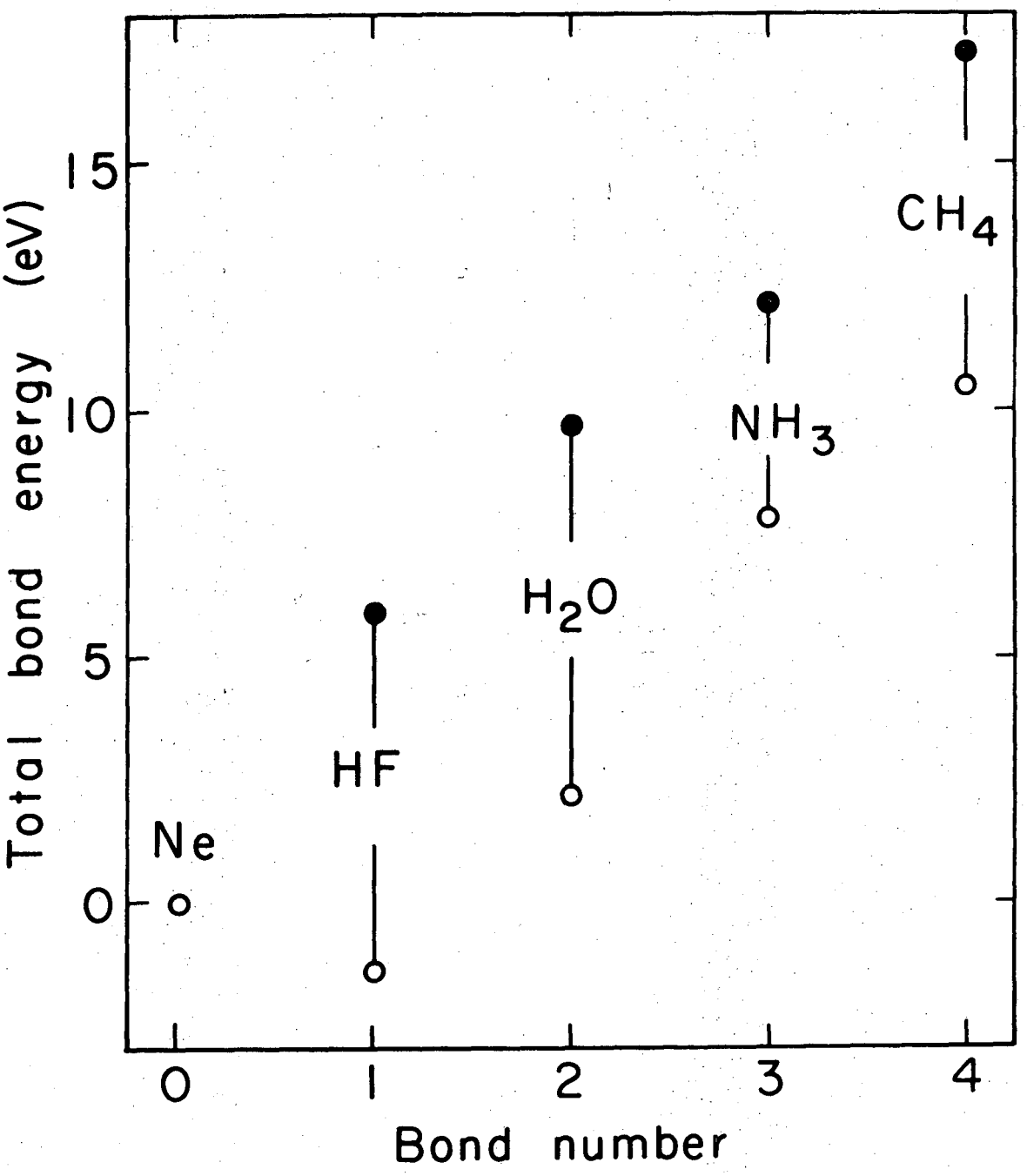

XBL754-2700

Fig. 4

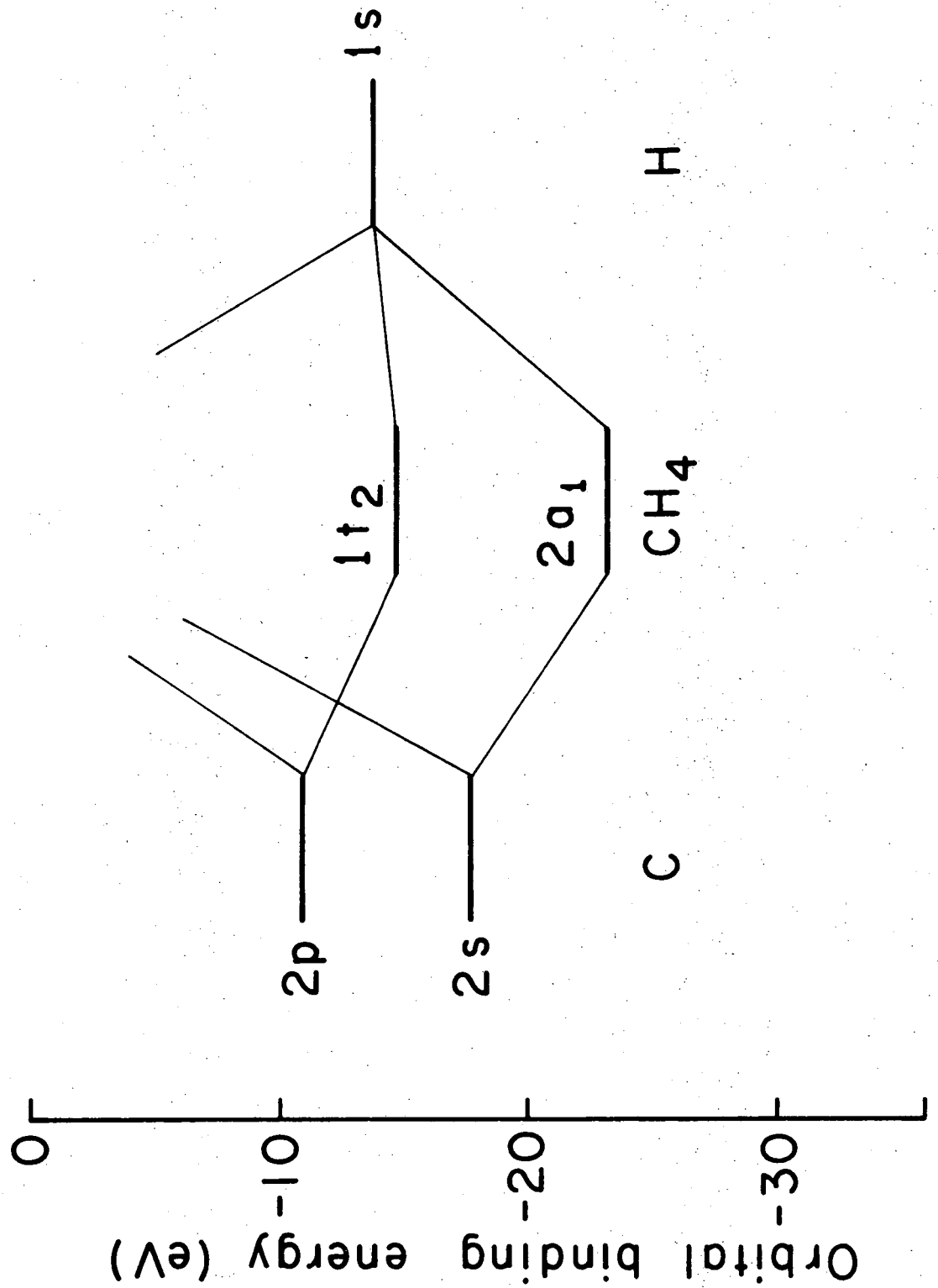

XBL754-2698

Fig. 5

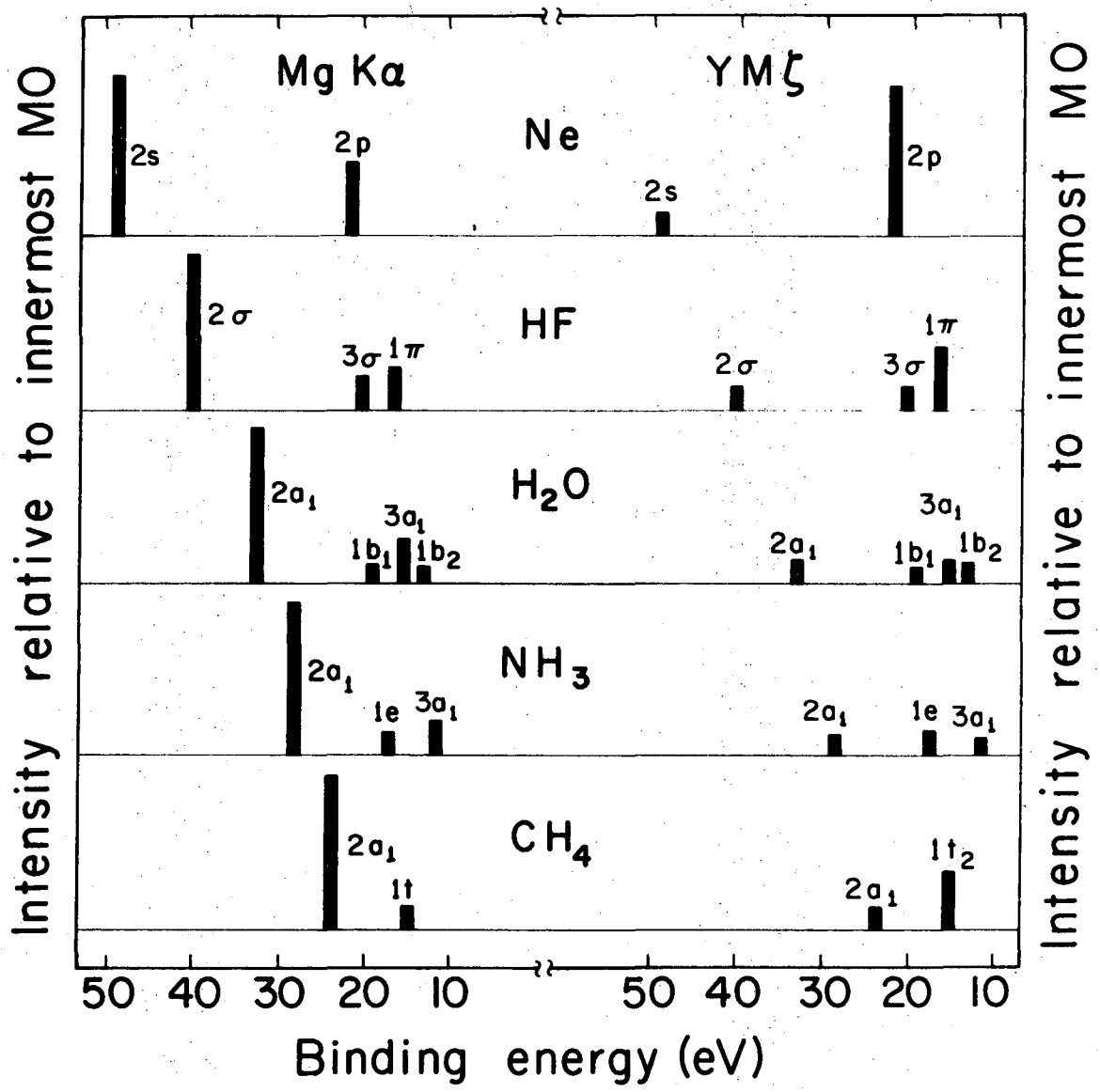

XBL754-2699

Fig. 6

TECHNICAL INFORMATION DIVISION
LAWRENCE BERKELEY LABORATORY
UNIVERSITY OF CALIFORNIA
BERKELEY, CALIFORNIA 94720